doi:10.1093/brain/awl135 *Brain* (2006), **129**, 1972–1983

A new focal EAE model of cortical demyelination: multiple sclerosis-like lesions with rapid resolution of inflammation and extensive remyelination

Doron Merkler,[1,*] Tristan Ernsting,[1,*] Martin Kerschensteiner,[3] Wolfgang Brück[1,2,†] and Christine Stadelmann[1,†]

[1]Department of Neuropathology, Georg-August University, Göttingen, [2]Institut für Multiple-Sklerose-Forschung, Bereich Humanmedizin der Georg-August Universität Göttingen und Gemeinnützige Hertie-Stiftung, Göttingen and [3]Research Unit 'Therapy Development', Institute of Clinical Neuroimmunology, Ludwig-Maximilians-University, Munich, Germany

Correspondence to: Prof. Dr Wolfgang Brück, Department of Neuropathology, Georg August University Göttingen, Robert-Koch-Strasse 40, 37075 Göttingen, Germany
E-mail: wbrueck@med.uni-goettingen.de
[*]These authors contributed equally to this work as co-first authors.
[†]These authors contributed equally to this work as co-senior authors.

Recent studies have revealed widespread demyelination in the cortex of patients with chronic multiple sclerosis. In contrast to white matter lesions, cortical multiple sclerosis lesions are accompanied by only minor inflammation. Research into the pathogenesis of cortical lesion formation has been hampered by the fact that the conventional rodent model of multiple sclerosis, experimental autoimmune encephalomyelitis (EAE), does not regularly affect the cortex. To overcome this limitation we developed a new rat model of cortical multiple sclerosis. Lesions were stereotactically targeted to the cerebral cortex by injection of pro-inflammatory mediators in animals that were immunized subclinically with myelin oligodendrocyte glycoprotein (MOG). We thus generated highly reproducible demyelinated lesions in the neocortex with remarkable histological similarities to cortical multiple sclerosis lesions. The focal cortical EAE model led to the typical pattern of intracortical and subpial demyelination, infiltration with inflammatory cells, complement deposition, acute axonal damage and neuronal cell death. Surprisingly, extensive cortical inflammation largely resolved within 2 weeks. Furthermore, cortical demyelination was readily compensated by rapid remyelination. Our data thus suggest that cortical inflammation is a transient phenomenon, and that remyelination of cortical inflammatory-demyelinating lesions may occur rapidly.

Keywords: neuroinflammation; multiple sclerosis; neuroimmunology; cortex; EAE

Abbreviations: APP = amyloid precursor protein; EAE = experimental autoimmune encephalomyelitis; IFA = incomplete Freund's adjuvant; MOG = myelin oligodendrocyte glycoprotein; PBS = phosphate-buffered saline.

Received February 8, 2006. Revised April 21, 2006. Accepted April 24, 2006. Advance Access publication May 19, 2006.

Introduction

Multiple sclerosis is the most common chronic neurological disease of young adulthood. Multiple demyelinated lesions disseminated throughout the white matter of the CNS are the pathological and radiological hallmarks of this disease. These lesions are histopathologically characterized by demyelination, inflammation, relative axonal preservation and gliosis (Prineas, 1985; Lassmann, 1998). Recently, pathological studies have revealed a prominent involvement of the cerebral cortex in patients with chronic multiple sclerosis (Kidd *et al.*, 1999; Bo *et al.*, 2003*b*). Cortical lesions were classified on the basis of their topographical localization, that is, cortico-subcortical, intracortical or subpial (Kidd *et al.*, 1999; Peterson *et al.*, 2001). The most common cortical lesion type was found to spread subpially, involving many adjacent gyri (Bo *et al.*, 2003*b*). Furthermore, apoptotic neurons and transected neurites were described in cortical lesions of patients (Peterson *et al.*, 2001). In a recent study, it was suggested that cortical lesions contribute to clinical

symptoms and disease progression in chronic multiple sclerosis (Kutzelnigg *et al.*, 2005).

White matter multiple sclerosis lesions are thought to arise through T-cell-mediated inflammation along with antibody/complement and macrophage-mediated destruction of myelin sheaths, or primary dysfunction of the myelin/oligodendrocyte unit (Lucchinetti *et al.*, 2000; Stadelmann *et al.*, 2005). The pathogenesis of cortical lesions in human multiple sclerosis, however, is largely unknown. Cortical lesions typically show less inflammation than white matter lesions (Peterson *et al.*, 2001; Bo *et al.*, 2003*a*). It has been proposed that demyelination caused by an antibody/complement attack or an unknown inflammatory mediator could play a role (Schwab and McGeer, 2002; Bo *et al.*, 2003*a*). However, the extent of complement deposition in purely cortical lesions has not been found to be significantly increased compared with non-demyelinated grey matter (Brink *et al.*, 2005).

These location-dependent differences between white matter and cortical lesions could be explained by regional differences in pathogenesis on the one hand. On the other, the local microenvironment could influence the degree of inflammation, tissue damage and repair—despite the underlying pathogenesis being identical. It is currently not clear whether cortical demyelination evolves in the absence of inflammation or whether inflammation and complement deposition are short-lived phenomena during early stages of cortical lesion formation.

The elucidation of pathomechanism(s) leading to cortical demyelination in multiple sclerosis is at present hampered by the lack of useful animal models reflecting human cortical pathology. This can be ascribed to the fact that rodent experimental autoimmune encephalomyelitis (EAE), the most widely used animal model for multiple sclerosis, rarely affects the brain. Neocortical demyelination reflecting the topographically different cortical lesion subtypes in multiple sclerosis has recently been described in the marmoset (*Callithrix jacchus*) EAE model (Pomeroy *et al.*, 2005; Merkler *et al.*, 2006). However, owing to the highly demanding requirements for infrastructure and animal husbandry, a more widely applicable EAE model mimicking human cortical multiple sclerosis pathology is still needed. Intracerebral injections of pro-inflammatory cytokines have been shown to augment the inflammatory response in the CNS of rodents immunized with guinea pig spinal cord homogenate (Sun *et al.*, 2004). In the present study, we have adapted a previously established targeted spinal EAE model (Kerschensteiner *et al.*, 2004*b*) for the induction of cortical lesions. Stereotactical injections of pro-inflammatory cytokines into the cortex of Lewis rats immunized with a subthreshold dose of myelin oligodendrocyte glycoprotein (MOG) led to the formation of reversible cortical demyelination sharing striking similarities with human cortical multiple sclerosis lesions. This model allowed us to study the pathogenetic events resulting in cortical pathology in a precise, temporally well-defined manner.

Material and methods

Animals

The experiments were carried out in adult (140–220 g) female Lewis rats obtained from Harlan (Horst, Netherlands). The animals were kept in groups on a 12 : 12 h light/dark cycle with food and water *ad libitum*. All experiments were approved by the Bezirksregierung Braunschweig, Germany.

Sensitization procedure

For induction of targeted EAE, recombinant MOG (rMOG) corresponding to the N-terminal sequence of rat MOG (amino acids 1–125) was expressed in *Escherichia coli* and purified to homogeneity as described previously (Adelmann *et al.*, 1995). The purified protein was dissolved in 6 mol/l of urea and dialysed against 20 mmol/l of sodium acetate buffer (pH 3.0) to obtain a soluble preparation and stored at −20°C.

Rats (n = 74) were anaesthetized by inhalation anaesthesia and injected subcutaneously at the base of tail with a total volume of 100 μl of rMOG (50 μg MOG diluted in saline) emulsified in incomplete freund's adjuvant (IFA; Sigma-Aldrich, Buchs, Switzerland). For control experiments, rats (n = 32) were injected subcutaneously at the base of tail with a total volume of 100 μl of saline emulsified in IFA. Healthy, age-matched animals (n = 4) without any treatment were used as a further control group for axon counts on histological sections (*see* below). For the induction of a targeted EAE lesion, MOG-sensitized rats were kept for 18–22 days and then were given a stereotactic injection of cytokines into a predetermined location of the cerebral cortex (*see* below).

Intracerebral stereotactic injection

Sensitized rats were anaesthetized by isoflurane inhalation anaesthesia and mounted in a stereotactic device. A fine hole was drilled through the skull giving access to the surface of the brain 1 mm caudal to the bregma and 2 mm lateral to the sagittal suture. A finely calibrated glass capillary was then stereotactically inserted, targeting the cortex (~1.5 mm depth). The rats were then injected with 1 μl of a cytokine mixture composed of 250 ng of recombinant rat tumour necrosis factor-α (TNF-α; R&D Systems, Abingdon, UK) and 150 U of recombinant rat interferon-γ (IFN-γ; PeproTech, London, UK) dissolved in phosphate-buffered saline (PBS) over a 3 min period. In a subset of MOG-primed animals (n = 6), stereotactic injections were performed with 1 μl of PBS only. A trace of monastral blue (Sigma-Aldrich) was added as a marker dye for better visibility. After injection the glass capillary was carefully withdrawn and the operation site was sealed by suture. Post-surgical recovery was uneventful in all cases, with no overt clinical signs.

Enzyme-linked immunosorbent assay

For the determination of serum titres of anti-MOG antibodies, blood samples were taken by puncture of the sublingual veins. After centrifugation of the blood samples the serum was separated and the titre of MOG-specific antibodies was determined by enzyme-linked immunosorbent assay (ELISA) as described earlier (Kerschensteiner *et al.*, 2004*b*). Briefly, recombinant purified MOG (rMOG) corresponding to the N-terminal sequence of rat MOG was coated on a 96-well Maxi Sorp plate (Nunc, Wiesbaden, Germany) at a concentration of 8 μg/ml. After incubation overnight at 4°C the plates were blocked with 5% (w/v) bovine serum albumin (BSA; SERVA, Heidelberg, Germany) in PBS for 4 h at room temperature.

Sera were pre-diluted 40-fold and then titrated in 3-fold dilutions throughout 12 steps in 5% (w/v) BSA in PBS. Detection was carried out with IgG-specific horseradish peroxidase-conjugated goat anti-rat antibodies (1 : 5000; Pierce, Rockford, IL, USA) in PBS with 0.1% (v/v) Tween-20 (Merck, Darmstadt, Germany) and 0.05% (w/v) BSA, with 3,3′-5,5′-tetramethylbenzidine (BM-Blue, POD; Rôche, Basel, Switzerland) added as a substrate. Between each incubation step, the plates were washed five times with PBS containing 0.05% (v/v) Tween-20. Optical density was measured at 450 nm. Antibody titres were defined as the serum dilutions yielding absorption of 2-fold background levels.

Histopathology and immunohistochemistry

The animals received an overdose of xylazine/ketamine after various survival times following cytokine injection (1, 3, 7 and 14 days after cytokine injection). The brains were dissected and fixed in HOPE fixative (DCS Innovative, Germany) overnight followed by tissue dehydration with acetone as described earlier (Olert *et al.*, 2001). A subset of animals was perfused transcardially with 4% paraformaldehyde. Fixed brain tissues were embedded in paraffin.

Histological evaluation was performed on 3-μm-thick sections stained with haematoxylin and eosin (H&E), Luxol fast blue/periodic acid Schiff agent (LFB/PAS) and Bielschowsky silver impregnation to assess inflammation, demyelination and axonal pathology, respectively. In adjacent serial sections, immunohistochemistry was performed using antibodies for macrophages/activated microglia (clone ED1; Serotec, Oxford, UK), $CD4^+$ T helper cells (Clone 15-8A2, HyCult Biotechnology b.v., Netherlands), $CD8^+$ cytotoxic T cells (Clone MCA 48R, Serotec), myelin basic protein (MBP, A0623; DakoCytomation), amyloid precursor protein (APP, clone 22C11; Chemicon, Temecula, CA, USA) as a marker for acute axonal damage, activated caspase-3 (CM1, rabbit polyclonal, IDUN Pharmaceuticals, La Jolla, CA, USA) to detect apoptotic cells, anti-neuronal nuclei NeuN (Chemicon International, Temecula, CA, USA) as a marker of neurons, and Nogo-A [mAb 11C7 (Oertle *et al.*, 2003), kindly provided by M. E. Schwab, Brain Research Institute, Department of Neuromorphology, University and ETH Zurich] as a marker for oligodendrocytes. Deposition of complement was detected with rabbit anti-rat C9 antibody (1 : 1000, kindly provided by Dr P. Morgan, Department of Biochemistry, Cardiff, UK). Bound antibodies were visualized using an avidin–biotin technique with 3, 3′-diaminobenzidine as chromogen.

Double-labelling immunohistochemistry for light microscopy was performed by visualizing the first primary antibody using DAB as a chromogen, followed by detection of the second primary antibody using an alkaline phosphatase anti-alkaline phosphatase technique with Fast Red. For fluorescence double-labelling bound antibody was visualized with Cy3- or Cy2-conjugated goat-anti rabbit IgG and donkey anti-mouse IgG (both from Jackson ImmunoResearch, Cambridgeshire, UK) with DAPI (Sigma-Aldrich) nuclei counterstaining.

TUNEL staining was performed according to the manufacturer's instructions using a kit from Roche Applied Systems (Hoffmann-La Roche AG, Grenzach-Qyhlen, Germany). Briefly, deparaffinized sections were incubated for 1 h at 37°C with a reaction mix containing 10 μl tailing buffer, 2 μl cobalt chloride, 1 μl digoxigenin labelling mixture and 6 units terminal transferase in a total volume of 50 μl. After a washing step, sections were incubated with an alkaline phosphatase-labelled anti-digoxigenin antibody for 1 h at room temperature. The colour reaction was performed with nitroblue tetrazolium (NBT) and 5-bromo-4-chloro-3-indolylphosphate (BCIP).

Morphometric analysis

Light microscopy

Adjacent 3-μm coronal serial sections were obtained from rostrocaudal levels of the forebrain (+0 to −3 mm). Every tenth section was stained for HE, and the epicentre of the injection site was determined for each animal. Sections adjacent to the injection site were then used for further histomorphological analysis.

In sections stained for ED1 and CD4, cortical vessels showing endothelial adhesion and perivascular infiltration were counted for the injected hemisphere. Densities of perivascular immunolabelled cells (within three cell layers around a vessel) as well as those of immunolabelled cells located within the brain parenchyma (located distant to three cell layers from a cortical vessel) were then quantified using an ocular morphometric grid at ×400 magnification. For each section, both perivascular density and invasion into the brain parenchyma were determined for the 10 cortical vessels with the highest density of inflammatory cells. The mean number of cells per square millimetre is given.

Digital images of tissue sections were recorded through an Olympus light/fluorescent microscope (Olympus Optical Co. Ltd) with a CCD camera (Color View II, Soft imaging System®, Münster, Germany). The extent of demyelination (in square millimetres) was then quantified by measuring the lesion area on overview photographs (×40) of MBP-immunostained sections using the Analysis Software Color View II (Soft imaging System®).

Densities of Nogo-A^+ oligodendrocytes were determined within the injected hemisphere both in cortical layers III–V (within the affected cortex) and layer VI (beyond cortical demyelination). For this purpose, the number of immunolabelled cells within 10 optical fields at a ×400 magnification was quantified for each animal and location using a counting grid. Oligodendrocyte cell densities in the corresponding area of the non-injected hemisphere were used as an internal control and set as 100%.

The axonal density of cerebral cortex layer III was determined in sections stained with Bielschowsky's silver impregnation 14 days after cytokine injection in animals immunized with MOG/IFA or IFA alone using a 24-point eye-piece. Histological sections of untreated age-matched animals served as a (further) control group.

Electron microscopy

In a subset of animals, electron microscopic analysis was carried out to determine the extent of remyelination in proximity to the injection site (corresponding to cortical layers III–V). MOG-primed animals received an overdose of xylazine/ketamine and were transcardially perfused with 3% glutaraldehyde in phosphate buffer 14 days after cytokine injection and post-fixed for at least 48 h ($n = 2$). Each brain was then dissected and cut coronally through the injection site. Para-sagittal slices of 1-mm thickness were obtained and trimmed. The regions of interest were processed through osmium tetroxide, dehydrated and embedded in Araldite. Semithin sections were stained with toluidine blue to identify the injection site by light microscopy. Ultrathin sections were then cut for electron microscopy. Age-matched, MOG-primed animals without cytokine injection ($n = 2$) served as controls and were processed identically.

The injection site was localized at low magnification in the electron microscope (×5000) before systematically recording images of the surrounding cortical grey matter at ×10000 magnification using a CCD camera (MegaView III, Soft Imaging System®). Pictures from control animals were recorded at the corresponding anatomical location. An area of at least 8×10^8 nm^2 was analysed per animal. Axon diameters and myelin sheath thicknesses of at least 220 myelinated axons (>0.2 μm in diameter) were measured per animal. Subsequently, the g-ratio (axon diameter/fibre diameter) was calculated as described previously (Coetzee *et al.*, 1996). Additionally, the axon density of myelinated fibres (>0.2 μm in diameter) within the measured area was determined and expressed as axons per square millimetre.

Statistical analysis

Data were analysed using SPSS Version 11 for Windows. Graphs were generated using GraphPad Prism version 4.00 for Windows (GraphPad Software, San Diego, CA, USA). Statistical analyses included one-way ANOVA (analysis of variance) followed by multiple Fisher's post-*t*-tests if the *F*-test of ANOVA indicated statistically significant differences.

Results

Cortical demyelination in targeted EAE mimics cortical multiple sclerosis lesions

Before stereotactic cytokine injection, animals were immunized subcutaneously either with MOG emulsified in IFA or with IFA alone. To monitor the immune response against MOG, serum antibody titres were determined by ELISA 3 and 5 weeks after immunization in a subset of animals (Fig. 1). Three days after intracortical injection with IFN-γ and TNF-α, extensive subpial demyelination was observed by MBP immunohistochemistry in the ipsi-, but not in the contralateral, non-injected hemisphere in MOG-primed animals (Fig. 2A and B; inset 1 in Fig. 2B). In contrast, IFA-immunized animals that were injected intracortically with the same cytokine mixture did not reveal any demyelination (inset 'IFA' in Fig. 2B). Intracortical injection of PBS alone in a subset of MOG-immunized animals ($n = 6$) demonstrated only marginal demyelination confined to the proximity of the needle track 3 days after injection (data not shown).

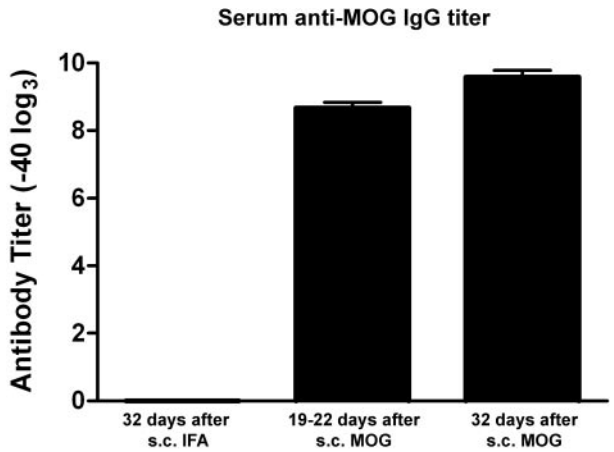

Fig. 1 Titres of anti-MOG antibodies. High and consistent anti-MOG antibody titres were detectable by ELISA in rats 19–22 or 32 days after subcutaneous (s.c.) immunization with 50 μg of MOG emulsified in IFA. Subcutaneous injection of IFA alone did not reveal a significant antibody response against MOG 32 days after immunization ($n = 4$–6 animals per group and time point; data are means + SEM).

In MOG-primed animals with cytokine injection, the topography of extensive subpial demyelination was highly reminiscent of cortical type III lesions (Peterson *et al.*, 2001) found in multiple sclerosis autopsy tissue (inset 'MS autopsy' in Fig. 2B). In addition, we detected purely intracortical demyelinated lesions, which were smaller, round to oval in shape and always centred on a vessel (inset 2 in Fig. 2B). Subpial lesions accounted for ~90% of the total demyelinated area at the peak of demyelination. As early as Day 1 (Fig. 3A, upper panel), but most prominently on Day 3 (Fig. 3A, lower panel) after cytokine injection, lesions contained macrophages/microglia cells, which had ingested MBP$^+$ fragments, as evidence for ongoing demyelination in the cerebral cortex. Furthermore, perivascular deposition of complement was detectable at sites of ongoing demyelination compatible with an involvement of antibody- and complement-mediated mechanisms (Fig. 3C). The time course of cortical demyelination parallelled that of the inflammatory infiltration with a peak on Day 3 as described in detail below (Fig. 3D–F).

Cortical inflammation peaks early and resolves within one week after cytokine injection

On Day 1 after cytokine injection, both MOG/IFA- and IFA-immunized animals had vessels displaying endothelial adhesion of CD4$^+$ T cells. In MOG/IFA-primed animals, however, the number of intracortical vessels with endothelial adhesion of CD4$^+$ T cells (26.7 ± 3.9 vessels, ipsilateral cortex, $n = 6$) significantly exceeded those of animals immunized with IFA alone (4.8 ± 1.6, $n = 4$, $P < 0.01$). Similarly, densities of perivascular and parenchymal CD4$^+$ T cells were significantly higher in MOG-primed animals compared with IFA controls (Fig. 4A left panel: MOG, right panel: IFA; Fig. 4J and K). Densities of parenchymal CD4$^+$ T cells rose considerably from Day 1 to Day 3 after cytokine injection in MOG/IFA-immunized animals (Fig. 4K). Notably, perivascular and parenchymal infiltration by CD4$^+$ T cells were transient and dropped sharply from Day 3 to Day 7 (Fig. 4B and C). CD4$^+$ T cells were also detectable in the ipsilateral cortical meninges and at the tip of the needle track by Day 1 after cytokine injection (data not shown). In animals pre-immunized with IFA alone, only a few CD4$^+$ T cells were found perivascularly as well as in the ipsilateral meninges and in close vicinity to the needle track (Fig. 4A, right panel and data not shown). The density of CD4$^+$ T cells correlated

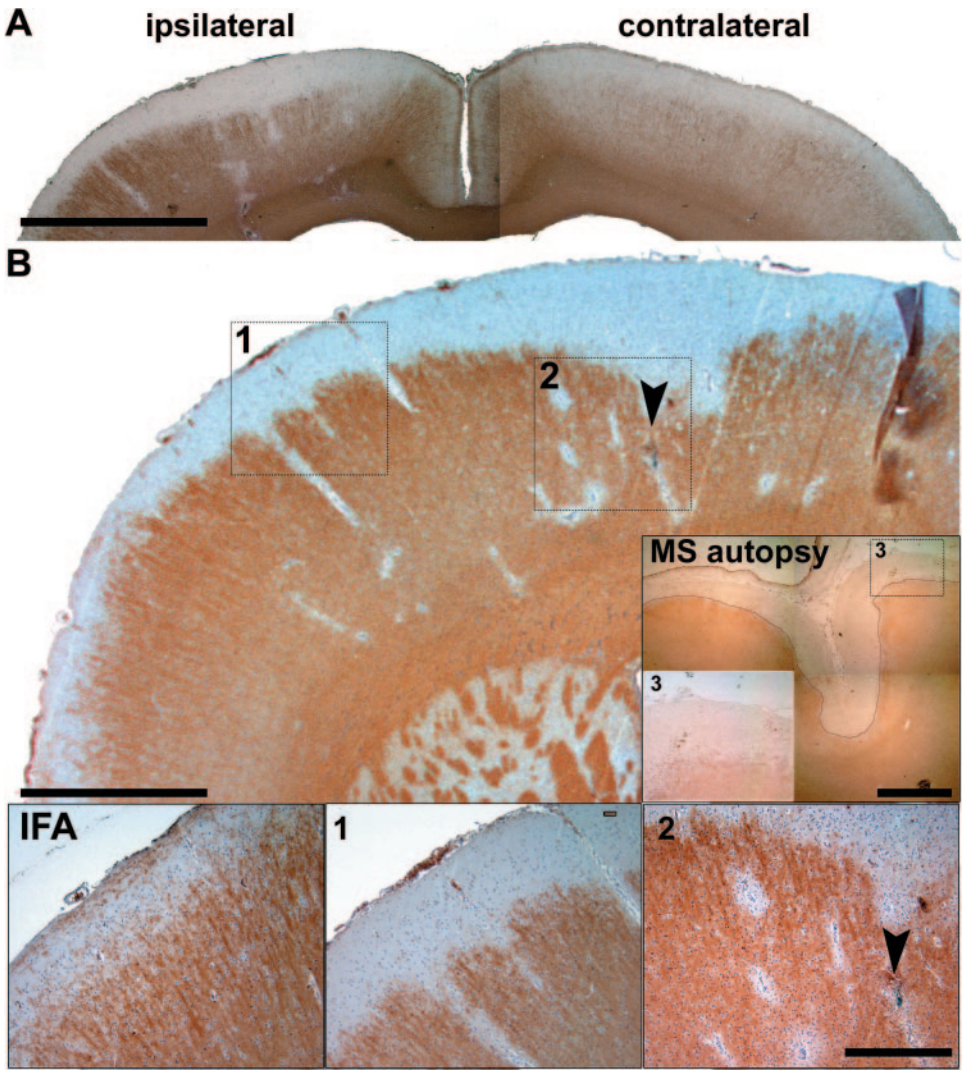

Fig. 2 Cortical demyelination in targeted EAE mimics cortical multiple sclerosis pathology. (**A**) Representative overview micrograph showing cortical demyelination by loss of MBP immunoreactivity ipsilateral to the cytokine injection. Note that the contralateral hemisphere does not show any signs of demyelination. (**B**) Representative ipsilateral brain section of a MOG-primed rat 3 days after pro-inflammatory cytokine injection stained for MBP. Extensive demyelination is apparent subpially (inset 1) and around numerous vessels (inset 2) within the cerebral cortex. Subpial demyelination in targeted cortical EAE lesions is highly reminiscent of subpial demyelination found in MS autopsy (inset 'MS autopsy'; line marks border of demyelination). Animals immunized with IFA alone did not reveal demyelination upon pro-inflammatory cytokine injection (inset 'IFA'). Arrowhead in inset 2 (**B**) indicates the site of cytokine injection (traces of monastral blue). Original magnifications: ×20 (**A** and inset 'MS autopsy' in **B**), ×40 (**B**); ×100 (insets 1, 2 and 'IFA' in **A**). Scale bars: 2000 μm (**A** and inset 'MS autopsy' in **B**), 1000 μm (**B**), 100 μm (inset 2 in **B**). MS = multiple sclerosis.

moderately but significantly with the extent of demyelination ($r = 0.45$, $P = 0.0008$).

$CD8^+$ cells were detected in cortical EAE lesions of MOG-primed animals up until Day 7 after cytokine injection with a peak on Day 3. (Fig. 4D–F). The quantification of $CD8^+$ T cells, however, was hampered by the fact that not only T cells but also cells displaying macrophage/microglia morphology showed surface expression of CD8 antigen. This phenomenon has been previously described in rat MOG EAE and focal brain ischaemia models (Schroeter *et al.*, 1999; Schroeter *et al.*, 2003). Expression of CD8 on macrophages/microglia cells was most prominent in MOG-primed animals 3 days after cytokine injection, suggesting an association of CD8 expression with the activation of macrophages/microglia cells (Fig. 4E). In animals immunized with IFA alone, only single $CD8^+$ cells were seen, almost exclusively in close proximity to the injection track on Day 1 after cytokine injection (data not shown).

On Day 1 after cytokine injection MOG-primed animals showed significantly more vessels with adhesion of $ED1^+$ cells (44.1 ± 2.9 vessels, ipsilateral cortex, $n = 12$; $P < 0.01$) than control animals (22.5 ± 1.8, $n = 4$). The considerable number of vessels with endothelial adherence of $ED1^+$ cells observed in the IFA-immunized group demonstrates

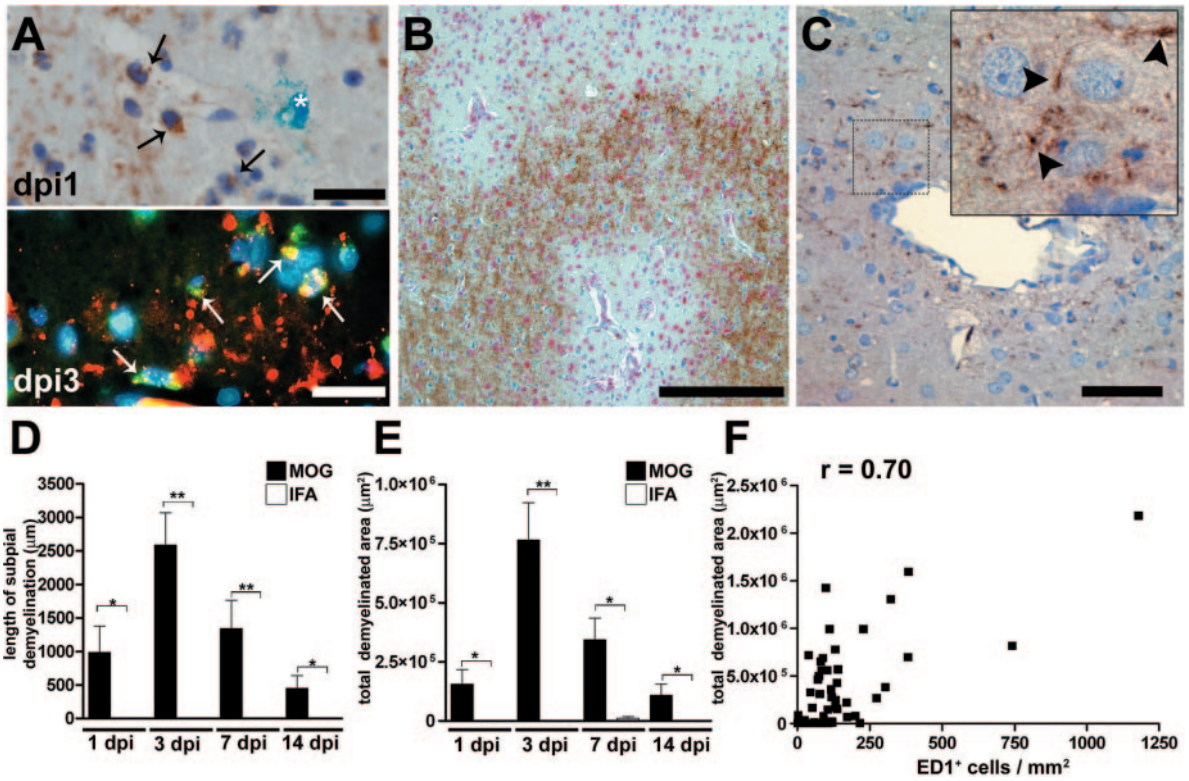

Fig. 3 Time-course analysis reveals rapid but transient cortical demyelinating activity in MOG-primed animals. (**A**, upper panel) High magnification of MBP-immunostained sections revealed MBP$^+$ myelin degradation products in macrophages (arrows) as early as Day 1 after cytokine injection (dpi), demonstrating ongoing demyelination. Traces of monastral blue (asterisk) indicate the cytokine injection site. (**A**, lower panel) Immunofluorescence double-labelling for MBP (red) and ED1$^+$ macrophages/microglial cells (green) at 3 dpi shows phagocytosed myelin debris within macrophages (arrows). Nuclei are visualized by DAPI counterstaining (blue). (**B**) Lower magnification of rat cortex co-stained for MBP (brown) and ED1 (red) reveals the relation between phagocytic infiltrates and demyelination at 3 dpi. (**C**) Perivascular C9-complement deposition suggests involvement of an antibody- and complement-mediated process. Length of subpial demyelination (**D**) and total area of cortical demyelination (**E**) in MOG- and IFA-immunized animals at 1, 3, 7 and 14 dpi. (**F**) Parenchymal ED1$^+$ cells correlate strongly with the extent of demyelination in MOG-primed animals over all time points examined [**D**: $n = 70$ animals, $r = 0.70$, $P < 0.0001$; r: correlation coefficient (Spearman rank test)]. Significant differences between groups are indicated as asterisk (*) for $P < 0.05$ and double asterisk (**) for $P < 0.01$. Data are expressed as mean + SEM ($n = 5$–15 per time point and group). Original magnifications: ×1000 (**A**), ×200 (**B**), ×400 (**C**). Scale bars: 20 µm (**A**), 200 µm (**B**), 50 µm (**C**).

that injection of pro-inflammatory cytokines alone is sufficient to cause adherence of blood-derived monocytes to cortical endothelia. In addition, both MOG/IFA- and IFA-injected animals harboured meningeal infiltrates of ED1$^+$ cells ipsilateral to the injection site already at Day 1 after cytokine injection (data not shown).

In MOG-primed animals, the perivascular density of ED1$^+$ cells remained constant from Day 1 to Day 3, followed by a steady decline until Day 14 (Fig. 4L). Of note, parenchymal ED1$^+$ cells were widely dispersed throughout the ipsilateral cortex, peaking at Day 3 after cytokine injection (Fig. 4H and M). In these animals, a spatiotemporal association between parenchymal ED1$^+$ cells and demyelination was observed (Fig. 3B), and the density of parenchymal ED1$^+$ cells strongly correlated with the extent of demyelination over all time points (Fig. 3F, $r = 0.7$, $P < 0.0001$). ED1$^+$ cells within the cerebral parenchyma were frequently stellate-shaped, reminiscent of activated microglia cells. The increase in density of ED1$^+$ cells was, however, as with T cells, short-lived with a peak on Day 3 after cytokine injection and rapidly declining thereafter (Fig. 4M).

In IFA-primed rats, ED1$^+$ infiltrates were restricted to the close proximity of the needle track and to perivascular areas after cytokine injection. In these animals, ED1$^+$ cells were much less dispersed into the parenchyma (Fig. 4L and M, data not shown). Furthermore, no foamy, myelin phagocytosing ED1$^+$ cells were observed.

Limited axonal damage and neuronal cell death in cortical EAE lesions

Previous studies have demonstrated axonal and dendritic transections as well as neuronal DNA fragmentation in cortical multiple sclerosis lesions (Peterson *et al.*, 2001; Vercellino *et al.*, 2005). In line with these findings, we observed APP$^+$ axonal spheroids indicative of acute axonal damage in our cortical EAE model (Fig. 5A–E). APP$^+$ axons in close proximity to the tip of the needle track were

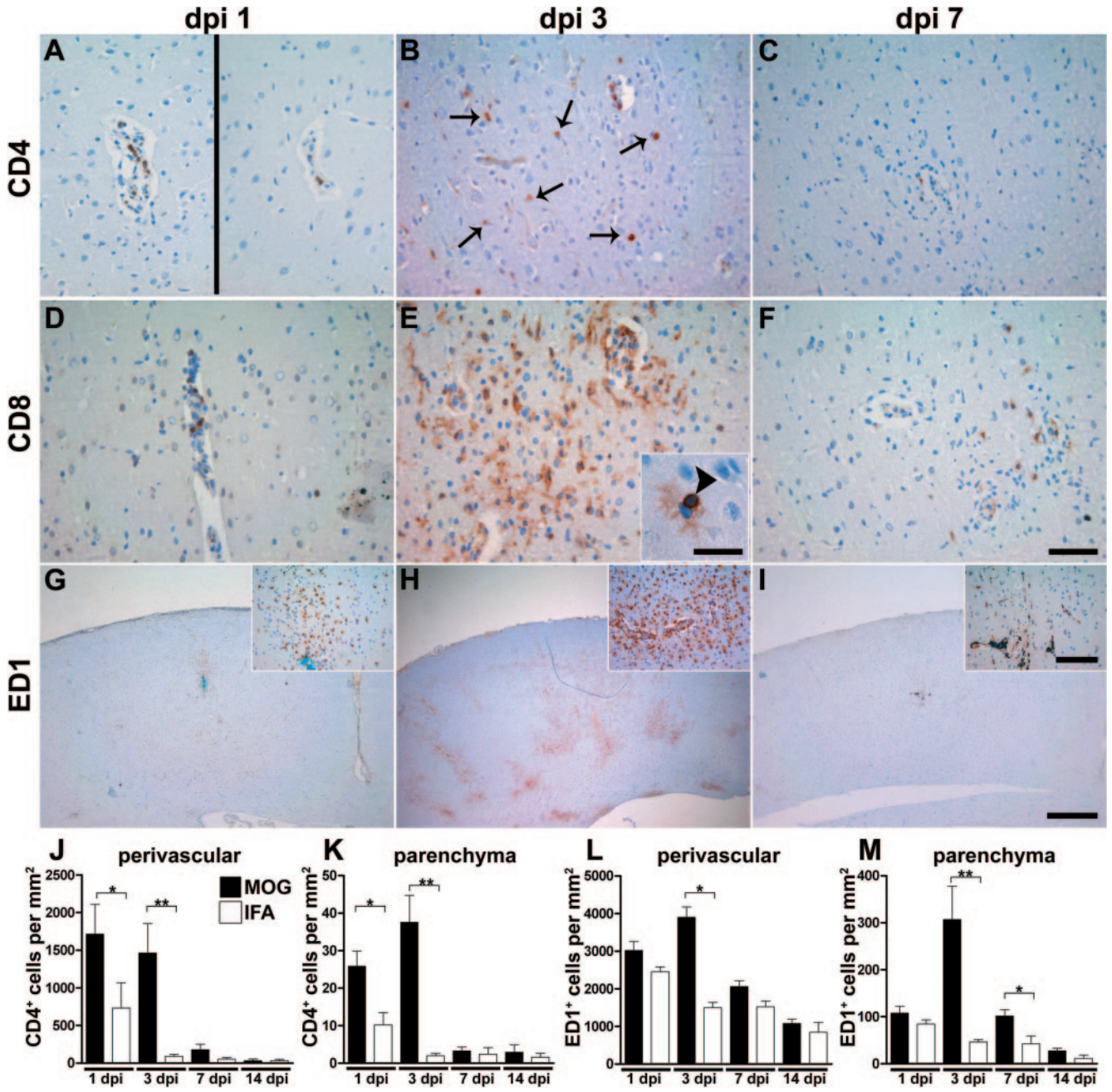

Fig. 4 EAE lesions targeted to the cerebral cortex of MOG-primed animals show an intense but transient inflammatory immune response upon injection of pro-inflammatory cytokines. Representative pictures 1 day (dpi 1; **A**, **D**, **G**), 3 days (dpi 3; **B**, **E**, **H**) and 7 days (dpi 7; **C**, **F**, **I**) after pro-inflammatory cytokine injection of animals immunized with 50 μg MOG in IFA. On Day 1 after cytokine injection of MOG-primed animals, numerous vessels show endothelial adhesion and perivascular accumulation of $CD4^+$ cells (left panel in **A**). Only a few vessels with single $CD4^+$ T-cell adhesion are observed in IFA-immunized animals (right panel in **A**). On Day 3 after cytokine injection of MOG-primed animals, $CD4^+$ T cells are scattered within the cortical parenchyma (**B**, arrows) with their numbers dropping sharply on Day 7 (**C**). Similar observations are made for cytotoxic $CD8^+$ T cells (**D**–**F**). On Day 3, numerous cells with microglia morphology express the CD8 antigen (**E**). Inset in **E** shows a $CD8^+$ cytotoxic T cell (arrowhead) in close proximity to a ramified microglia cell expressing the CD8 antigen. On Day 1 after cytokine injection, $ED1^+$ cells are detectable in the meninges, subpially, around numerous cortical vessels and in close proximity to the injection site (**G**). On Day 3 after cytokine injection, widespread infiltrates with $ED1^+$ cells are evident within the cortical parenchyma (**H**). On Day 7 after cytokine injection, only few $ED1^+$ cells are present, again mainly perivascularly and around the injection site (**I**). The quantification of perivascular and parenchymal $CD4^+$ and $ED1^+$ cell densities illustrates the kinetics of inflammatory infiltration (**J**–**K**). In animals immunized with IFA alone, perivascular accumulation of $CD4^+$ and $ED1^+$ cells is found primarily on Day 1 after cytokine injection. In contrast, the inflammatory response upon cytokine injection is much stronger and prolonged in MOG-primed animals. Values are expressed as mean + SEM. Significant differences between groups (MOG versus IFA) are indicated as asterisk (*) for $P < 0.05$ and double asterisk (**) for $P < 0.01$. Original magnifications: ×400 (**A**–**F** and insets in **G**–**I**); ×40 (**G**–**I**); ×1000 (inset in **E**). Scale bars: 50 μm (**F**); 20 μm (inset in **E**); 500 μm (**I**), 100 μm (inset in **I**).

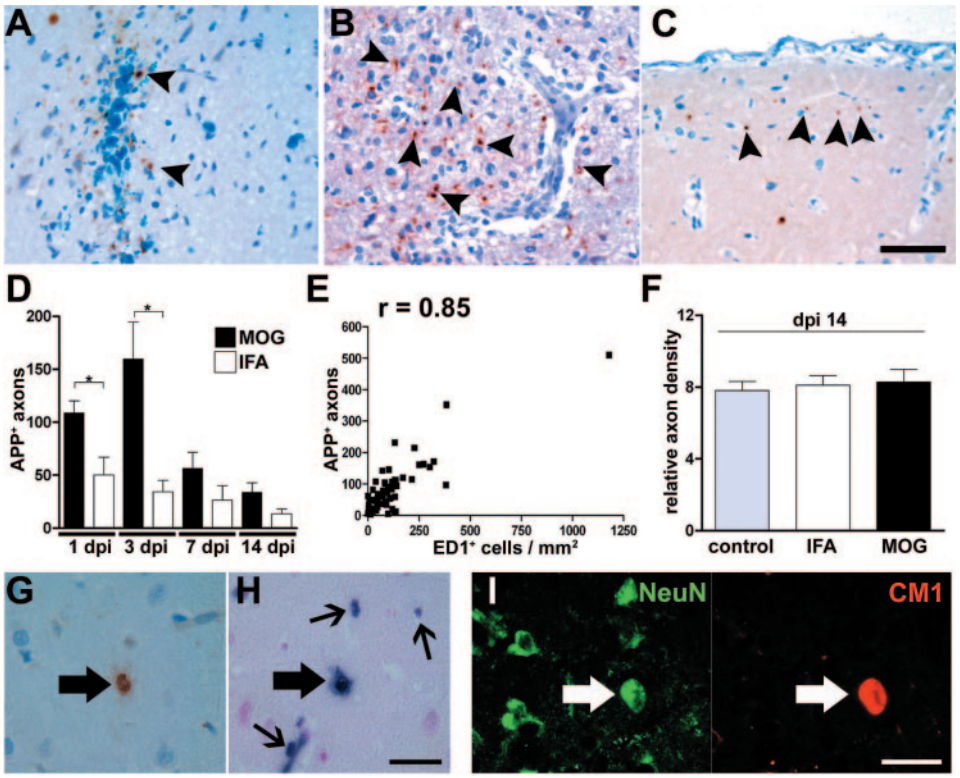

Fig. 5 Acute axonal damage and neuronal apoptosis in targeted cortical EAE lesions. (**A**–**C**) Immunohistochemical staining for APP, a marker for acute axonal damage. APP$^+$ spheroids (arrowheads in **A**) are detected in close proximity to the injection site (**A**) in both MOG/IFA-immunized and control (IFA) animals. In addition, numerous APP$^+$ axons are found in perivascular demyelinated and inflamed areas (**B**) and in areas of subpial demyelination (arrowheads in **C**) in MOG-primed animals, but not in controls. (**D**) Total number of APP$^+$ spheroids within the injected hemisphere in MOG/IFA- and IFA-immunized animals on Days 1, 3, 7 and 14 after lesion induction (dpi; n = 5–12 animals per time point and group). (**E**) The density of parenchymal ED1$^+$ cells correlates strongly with the number of APP$^+$ axons [n = 60 animals, r = 0.85, $P < 0.0001$; r: correlation coefficient (Spearman rank test)]. (**F**) Quantification of relative axonal densities in cortical layer III based on Bielschowsky silver impregnated sections did not reveal a reduction in axonal densities at 14 dpi in MOG/IFA- or IFA-primed animals compared with age-matched untreated controls (n = 4 animals per group). Immunohistochemical detection of activated caspase-3 (**G**) and TUNEL staining (**H**) 3 days after lesion induction in MOG-primed animals. Single apoptotic cells identified as neurons by their large nuclei (big arrow in **G** and **H**) and triangular cytoplasm are observed in areas of cortical demyelination. Numerous non-neuronal, presumably inflammatory or glial, cells are detected by TUNEL staining (small arrows in **H**). (**I**) Immunofluorescence staining reveals individual cells co-stained for neuron-specific antigen NeuN (green) and activated caspase-3 (red). Significant differences between groups (MOG and IFA) are indicated as asterisk (*) for $P < 0.05$; data are mean + SEM. Original magnifications: ×400 (**A**–**C**), ×1000 (**G** and **H**). Scale bar: 50 μm (**C**) and 20 μm (**H**).

observed in both MOG/IFA- and IFA-immunized animals (Fig. 5A). In MOG-primed animals, APP$^+$ axons were, furthermore, detectable around numerous inflamed intracortical vessels throughout the cortex (Fig. 5B) as well as in areas of subpial demyelination (Fig. 5C). The presence of APP$^+$ axons corresponded both in time and severity to that of the inflammatory infiltration. This is reflected in a significant correlation of APP$^+$ axons with the density of parenchymal ED1$^+$ cells (Fig. 5E; r = 0.85, $P < 0.0001$) and a weaker, but nonetheless highly significant, correlation with CD4$^+$ T cells (r = 0.48, P = 0.0014). The observed acute axonal damage did not, however, result in an apparent reduction in cortical axonal density 14 days after cytokine injection as determined by Bielschowsky's silver impregnation (Fig. 5F).

With regard to irreversible neuronal damage, only single neurons—identified by their triangular cytoplasmic shape and large nuclei—were highlighted by TUNEL (Fig. 5G) and by activated caspase-3 staining (Fig. 5H) at the peak of demyelination (3 days post-injection). Double immunofluorescence studies similarly marked single NeuN$^+$ neurons with anti-activated caspase-3 immunoreactivity (Fig. 5I).

Cortical demyelination in targeted EAE reveals extensive remyelinating capacity within the cerebral cortex

Two weeks after cytokine injection, only residual demyelination was detectable in the cerebral cortex of MOG-primed animals (*see* Fig. 3D and E). This pronounced reduction in

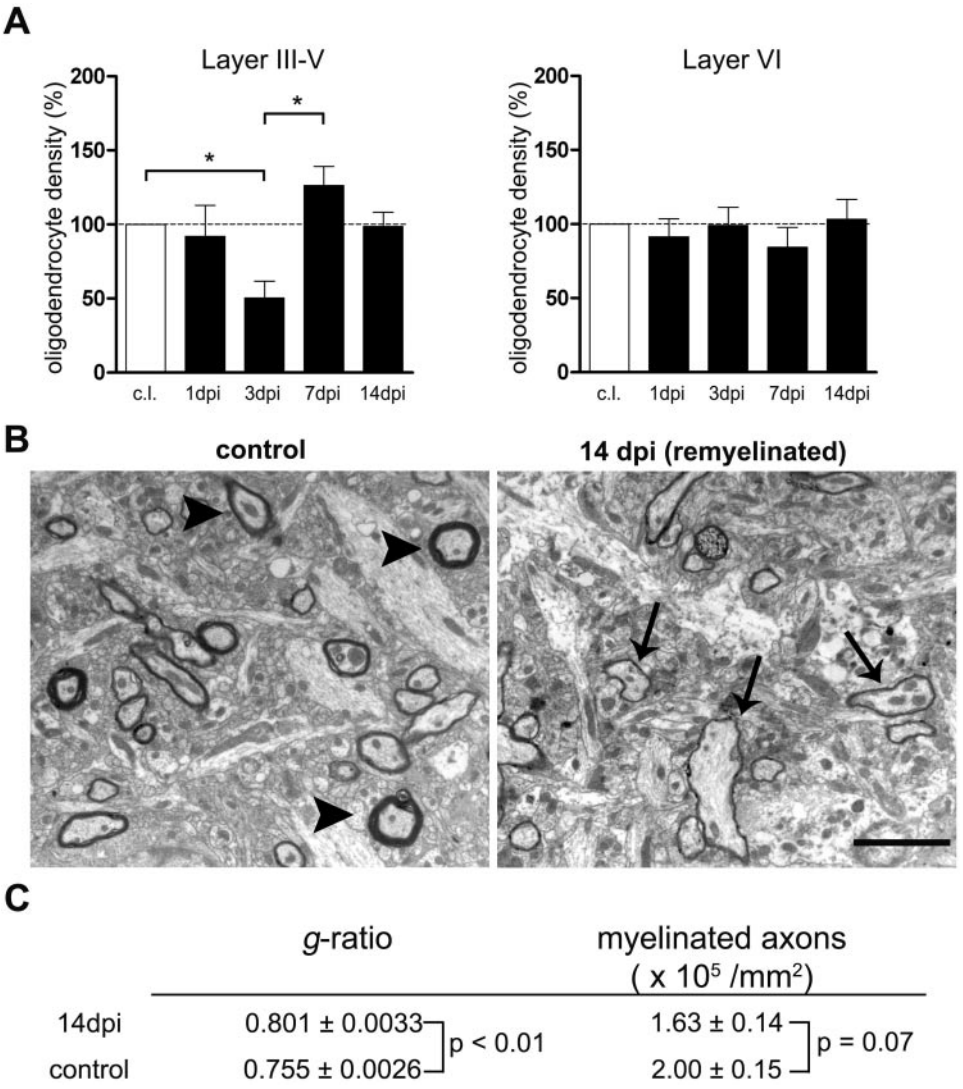

Fig. 6 Demyelinated cerebral cortex reveals repopulation with oligodendrocytes and extensive remyelination (**A**) Quantification of NogoA$^+$ oligodendrocyte density 1, 3, 7 and 14 days after cytokine injection in MOG-primed animals (n = 4–7 animals per time point) within cortical layers III–V (left panel) and layer VI (right panel). Corresponding contralateral (c.l.) oligodendrocyte densities are set as 100%. (**B**) Representative electron micrographs of control animals without demyelination (left panel) and from MOG-primed animals 14 days after cytokine injection (right panel). More axons display thinner myelin sheaths (arrows) in the latter group compared with control animals (arrow heads). (**C**) g-Ratios (axon diameter/total fibre diameter) are significantly higher in animals with previous cytokine injection (n = 455 scored axons of two animals) compared with control animals (n = 521 scored axons of two animals). No difference in densities of myelinated axons is observed between these two groups (P = 0.07). Data are mean ± standard deviation; original magnifications: ×10000 (**B**). Scale bar: 2 μm (**B**).

demyelinated area may suggest that a substantial number of axon fibres have been remyelinated.

Repopulation of demyelinated areas with oligodendrocytes represents a prerequisite for remyelination. We therefore performed immunostaining for Nogo-A, which marks oligodendrocyte cell bodies (Buss and Schwab, 2003). Three days after cytokine injection a reduction of ~50% of Nogo-A$^+$ oligodendrocytes was found within cortical layers III–V (Fig. 6A), parallelling the time point of most extensive demyelination as revealed by MBP immunostaining (*see* Fig. 3). By Day 7 after injection, oligodendrocyte numbers had increased significantly, even exceeding the density of oligodendrocytes in the contralateral cerebral cortex. Two weeks after cytokine injection, oligodendrocyte cell counts were again comparable with those of the contralateral cerebral cortex. Throughout the entire observation period the oligodendrocyte density of cortical layer VI (no demyelination) showed no significant change (Fig. 6A).

Characteristically, remyelinated axons display a reduction in the thickness of the myelin sheath in relation to their axon diameter when compared with normally myelinated axons. This results in an increase in the so-called g-ratio, a ratio of

axon to fibre diameter (Coetzee *et al.*, 1996). To analyse the extent of remyelination in cortical EAE lesions, we determined the g-ratios for myelinated axons in proximity to the injection site in electron micrographs of animals 14 days after cytokine injection as well as in non-injected controls ($n = 2$ per group, >220 myelinated axons per animal analysed) (Fig. 6B). We observed no significant difference in the cortical density of myelinated fibres between injected and control animals, although in injected animals, a trend toward lower densities was noted for injected animals ($P = 0.07$, Fig. 6C). However, numerous axons were found to have a reduction in myelin thickness in animals subjected to cytokine injection. Subsequent measurements revealed a highly significant increase in the g-ratio, providing evidence for remyelination ($P < 0.01$, Fig. 6C).

Discussion

In the present study, we describe a novel animal model of targeted cortical EAE that reproduces key features of human cortical demyelination in multiple sclerosis. Cortical demyelination is widespread in chronic patients and has been suggested to contribute to disease symptoms and progression. Via stereotactic cortical injection of cytokines into animals pre-immunized with MOG protein, we generated intracortical and subpial lesions with extensive demyelination and widespread but transient infiltration by T cells and macrophages/microglia cells. Furthermore, our results indicate an extensive remyelinating capacity of the cerebral cortex after inflammatory demyelination.

A striking phenomenon observed in the targeted cortical EAE lesion model is the transient nature of inflammatory infiltration and demyelination in the grey matter. This stands in contrast to EAE lesions targeted to the white matter of the spinal cord where dense infiltrates of macrophages/activated microglia persist over an observation period of 4 weeks without significant remyelination (Kerschensteiner *et al.*, 2004*a*, *b*). Notably, EAE lesions targeted to the subcortical white matter (corpus callosum) were similar to targeted white matter spinal cord EAE lesions with regard to persisting infiltration by inflammatory cells, demyelination and axonal damage (data not shown). This indicates that the immunopathology of an EAE lesion strongly depends on the site of lesion initiation, since priming with MOG and cytokine injection technique were identical in the above-mentioned experiments. The widespread infiltration seen in MOG-primed animals at early time points after lesion induction implies that the initial adhesion and infiltration of immune cells are not impaired in the cerebral cortex. This is in line with earlier findings, providing evidence that important adhesion molecules such as ICAM-1, VCAM and PECAM are either constitutively expressed on the cortical vasculature or upregulated upon inflammatory challenge (Bell and Perry, 1995). It could be speculated that the initial formation of cortical inflammatory demyelinated lesions in the targeted EAE model may be restricted in time and severity owing to different signals from the cortical microenvironment, for example, by distinct patterns of chemokine expression in cortex compared with white matter (Campbell *et al.*, 2002). Other explanations for differences in immunopathology include differences between cortex and white matter regarding macrophage/microglia activation, T-cell elimination, permeability of the blood–brain barrier (BBB), myelin content or composition and oligodendrocyte differentiation. The fact that inflammation resolves rapidly within the cortical microenvironment may account for the relative lack of inflammation typically found in chronically demyelinated cortical multiple sclerosis lesions (Bo *et al.*, 2003*a*).

Cortical demyelination in our model clearly depends on peripheral immune priming against a myelin protein (in this case MOG) since injection of pro-inflammatory cytokines in animals immunized with IFA alone was an insufficient trigger for cortical demyelination. However, cytokine injection was necessary in MOG-primed animals, since PBS injection alone caused only minor pathology. The detection of the complement component C9 within targeted cortical EAE lesions and the high antibody titres measured in the serum, furthermore, suggest an involvement of humoral immune mechanisms in cortical demyelination, similar to that proposed for a subgroup of white matter lesions in multiple sclerosis and EAE (Genain *et al.*, 1995; Storch *et al.*, 1998; Raine *et al.*, 1999; Archelos *et al.*, 2000; Lucchinetti *et al.*, 2000). However, C9 deposition was most pronounced in the first days after cytokine injection during ongoing cortical inflammation and demyelination. Our data suggest that complement deposition is only transiently detectable in cerebral cortex and could thus explain the reported lack of complement deposition in cortical lesions of multiple sclerosis autopsies (Brink *et al.*, 2005).

Previous studies have shown that molecular marker substances injected into the brain drain along perivascular spaces to the surface of the brain and even leak into the cerebrospinal fluid (Abbott, 2004). It is therefore likely that depending on the site of injection, cytokines distribute along predetermined anatomical routes. One could therefore speculate that cytokines injected intracortically are preferentially drained to subpial regions of the cerebral cortex and the meninges. Cytokines are known to cause BBB breakdown and to facilitate the influx of mononuclear cells (Simmons and Willenborg, 1990; Phillips and Lampson, 1999; Schnell *et al.*, 1999). In the setting of previous immune-priming against MOG, this drainage of intracortical pro-inflammatory cytokines might explain the distribution of the evolving EAE lesions. However, the observed pattern of demyelination is most likely not exclusively dependent on the presence of IFN-γ/TNF-α, and the injection or local expression of other pro-inflammatory cytokines or chemokines might result in similar EAE lesions in MOG primed animals.

Cortical demyelination was found to be a feature of progressive multiple sclerosis, but was rarely observed in patients with acute or relapsing disease (Kutzelnigg *et al.*, 2005).

Considering the high regenerative capacity of the cerebral cortex demonstrated by our targeted EAE model following a single episode of inflammatory demyelination, one might postulate that extensive and fast remyelination within the cerebral cortex may mask cortical demyelination in early multiple sclerosis. This is supported by the high propensity for remyelination observed in the majority of cortical multiple sclerosis lesions (M. Albert and C. Stadelmann, unpublished data). The presence of extensive cortical demyelination found in some chronic patients might represent an exhaustion of this remyelinating capacity, for example, by depletion of oligodendrocyte progenitor cells as has been postulated for white matter lesions (Johnson and Ludwin, 1981; Carroll *et al.*, 1998).

Neuronal death and axonal damage have recently been observed in cortical multiple sclerosis lesions (Peterson *et al.*, 2001). In our animal model acute axonal damage was most abundant at the peak of demyelination and inflammation on Day 3 after lesion induction. Nevertheless, axonal densities were not decreased within the targeted area of the cerebral cortex of either IFA- or MOG/IFA-immunized animals compared with healthy control animals 2 weeks after lesion induction. The presence of APP^{+} axons during the active phase of cortical demyelination may thus, in part, reflect reversible disturbances of axonal transport, which do not necessarily result in considerable axonal loss. Furthermore, as described for human cortical multiple sclerosis lesions, we identified single apoptotic neurons in acute cortical EAE lesions. Their number, however, was small and did not result in an apparent reduction of neuronal cell bodies following a single episode of demyelination.

In summary, we provide evidence that early demyelination in the cerebral cortex is associated with extensive, but short-lived, inflammation and deposition of complement C9, thus shedding light on the pathomechanisms operating in human cortical multiple sclerosis lesions. Furthermore, focal cortical EAE lesions show rapid and near-complete remyelination in concordance with our observations in human tissue. Our cortical EAE model thus reflects the key features of cortical multiple sclerosis lesions and provides a novel approach to study the evolution and resolution of cortical pathology. Owing to the defined time course and predetermined location of the lesion, our model may facilitate the elaboration of MRI parameters, allowing for a reliable *in vivo* detection of cortical pathology in multiple sclerosis and EAE. In addition, it may serve as a highly useful tool to test therapeutic approaches to multiple aspects of inflammatory demyelinating cortical pathology.

Acknowledgements

We would like to thank M. Schedensack and B. Maruschak for expert technical assistance. We would also like to thank Prof. M. E. Schwab and Prof. B. P. Morgan for providing us with antibodies. C.S. and W.B. hold grants from the Gemeinnützige Hertie-Stiftung. C.S. and D.M. are supported by the Medical Faculty of the University of Goettingen (junior research group). This work is also supported by 6th Framework Program of the European Union, NeuroproMiSe, LSHM-CT-2005-018637. T.E. was supported by the Deutsche Forschungsgemeinschaft (GRK 632 'Neuroplasticity'). M.K. is supported by the Emmy-Noether Programm of the DFG and the 'Verein Therapieforschung für MS-Kranke e.V'.

REFERENCES

Abbott NJ. Evidence for bulk flow of brain interstitial fluid: significance for physiology and pathology. Neurochem Int 2004; 45: 545–52.

Adelmann M, Wood J, Benzel I, Fiori P, Lassmann H, Matthieu JM, et al. The N-terminal domain of the myelin oligodendrocyte glycoprotein (MOG) induces acute demyelinating experimental autoimmune encephalomyelitis in the Lewis rat. J Neuroimmunol 1995; 63: 17–27.

Archelos JJ, Storch MK, Hartung H-P.. The role of B cells and autoantibodies in multiple sclerosis. Ann Neurol 2000; 47: 694–706.

Bell MD, Perry VH. Adhesion molecule expression on murine cerebral endothelium following the injection of a proinflammagen or during acute neuronal degeneration. J Neurocytol 1995; 24: 695–710.

Bo L, Vedeler CA, Nyland H, Trapp BD, Mork SJ. Intracortical multiple sclerosis lesions are not associated with increased lymphocyte infiltration. Mult Scler 2003a; 9: 323–31.

Bo L, Vedeler CA, Nyland HI, Trapp BD, Mork SJ. Subpial demyelination in the cerebral cortex of multiple sclerosis patients. J Neuropathol Exp Neurol 2003b; 62: 723–32.

Brink BP, Veerhuis R, Breij EC, van der Valk P, Dijkstra CD, Bo L. The pathology of multiple sclerosis is location-dependent: no significant complement activation is detected in purely cortical lesions. J Neuropathol Exp Neurol 2005; 64: 147–55.

Buss A, Schwab ME. Sequential loss of myelin proteins during Wallerian degeneration in the rat spinal cord. Glia 2003; 42: 424–32.

Campbell SJ, Wilcockson DC, Butchart AG, Perry VH, Anthony DC. Altered chemokine expression in the spinal cord and brain contributes to differential interleukin-1beta-induced neutrophil recruitment. J Neurochem 2002; 83: 432–41.

Carroll WM, Jennings AR, Ironside LJ. Identification of the adult resting progenitor cell by autoradiographic tracking of oligodendrocyte precursors in experimental CNS demyelination. Brain 1998; 121: 293–302.

Coetzee T, Fujita N, Dupree J, Shi R, Blight A, Suzuki K, et al. Myelination in the absence of galactocerebroside and sulfatide: normal structure with abnormal function and regional instability. Cell 1996; 86: 209–19.

Genain CP, Nguyen MH, Letvin NL, Pearl R, Davis RL, Adelman M, et al. Antibody facilitation of multiple sclerosis-like lesions in a nonhuman primate. J Clin Invest 1995; 96: 2966–74.

Johnson ES, Ludwin SK. The demonstration of recurrent demyelination and remyelination of axons in the central nervous system. Acta Neuropathol (Berl) 1981; 53: 93–8.

Kerschensteiner M, Bareyre FM, Buddeberg BS, Merkler D, Stadelmann C, Bruck W, et al. Remodeling of axonal connections contributes to recovery in an animal model of multiple sclerosis. J Exp Med 2004a; 200: 1027–38.

Kerschensteiner M, Stadelmann C, Buddeberg BS, Merkler D, Bareyre FM, Anthony DC, et al. Targeting experimental autoimmune encephalomyelitis lesions to a predetermined axonal tract system allows for refined behavioral testing in an animal model of multiple sclerosis. Am J Pathol 2004b; 164: 1455–69.

Kidd D, Barkhof F, McConnell R, Algra PR, Allen IV, Revesz T. Cortical lesions in multiple sclerosis. Brain 1999; 122: 17–26.

Kutzelnigg A, Lucchinetti CF, Stadelmann C, Bruck W, Rauschka H, Bergmann M, et al. Cortical demyelination and diffuse white matter injury in multiple sclerosis. Brain 2005; 128: 2705–12.

Lassmann H. Neuropathology in multiple sclerosis: new concepts. Mult Scler 1998; 4: 93–8.

Lucchinetti C, Bruck W, Parisi J, Scheithauer B, Rodriguez M, Lassmann H. Heterogeneity of multiple sclerosis lesions: implications for the pathogenesis of demyelination. Ann Neurol 2000; 47: 707–17.

Merkler D, Böscke R, Schmelting B, et al. Differential macrophage/microglia activation in neocortical EAE lesions in the marmoset. Brain Pathol. In press, 2006.

Oertle T, van der Haar ME, Bandtlow CE, Robeva A, Burfeind P, Buss A, et al. Nogo-A inhibits neurite outgrowth and cell spreading with three discrete regions. J Neurosci 2003; 23: 5393–406.

Olert J, Wiedorn KH, Goldmann T, Kuhl H, Mehraein Y, Scherthan H, et al. HOPE fixation: a novel fixing method and paraffin-embedding technique for human soft tissues. Pathol Res Pract 2001; 197: 823–6.

Peterson JW, Bo L, Mork S, Chang A, Trapp BD. Transected neurites, apoptotic neurons, and reduced inflammation in cortical multiple sclerosis lesions. Ann Neurol 2001; 50: 389–400.

Phillips LM, Lampson LA. Site-specific control of T cell traffic in the brain: T cell entry to brainstem vs. hippocampus after local injection of IFN-gamma. J Neuroimmunol 1999; 96: 218–27.

Pomeroy IM, Matthews PM, Frank JA, Jordan EK, Esiri MM. Demyelinated neocortical lesions in marmoset autoimmune encephalomyelitis mimic those in multiple sclerosis. Brain 2005; 128: 2713–21.

Prineas JW. The neuropathology of multiple sclerosis. In: Koetsier JC et al., editors. Demyelinating Diseases. Amsterdam: Elsevier Science Publishers; 1985. p. 213–57.

Raine CS, Cannella B, Hauser SL, Genain CP. Demyelination in primate autoimmune encephalomyelitis and acute multiple sclerosis lesions: a case for antigen-specific antibody mediation. Ann Neurol 1999; 46: 144–60.

Schnell L, Fearn S, Schwab ME, Perry VH, Anthony DC. Cytokine-induced acute inflammation in the brain and spinal cord. J Neuropathol Exp Neurol 1999; 58: 245–54.

Schroeter M, Jander S, Witte OW, Stoll G. Heterogeneity of the microglial response in photochemically induced focal ischemia of the rat cerebral cortex. Neuroscience 1999; 89: 1367–77.

Schroeter M, Stoll G, Weissert R, Hartung HP, Lassmann H, Jander S. CD8+ phagocyte recruitment in rat experimental autoimmune encephalomyelitis: association with inflammatory tissue destruction. Am J Pathol 2003; 163: 1517–24.

Schwab C, McGeer PL. Complement activated C4d immunoreactive oligodendrocytes delineate small cortical plaques in multiple sclerosis. Exp Neurol 2002; 174: 81–8.

Simmons RD, Willenborg DO. Direct injection of cytokines into the spinal cord causes autoimmune encephalomyelitis-like inflammation. J Neurol Sci 1990; 100: 37–42.

Stadelmann C, Ludwin S, Tabira T, Guseo A, Lucchinetti CF, Leel-Ossy L, et al. Tissue preconditioning may explain concentric lesions in Balo's type of multiple sclerosis. Brain 2005; 128: 979–87.

Storch MK, Stefferl A, Brehm U, Weissert R, Wallstrom E, Kerchensteiner M, et al. Autoimmunity to myelin oligodendrocyte glycoprotein in rats mimics the spectrum of multiple sclerosis pathology. Brain Pathol 1998; 8: 681–94.

Sun D, Newman TA, Perry VH, Weller RO. Cytokine-induced enhancement of autoimmune inflammation in the brain and spinal cord: implications for multiple sclerosis. Neuropathol Appl Neurobiol 2004; 30: 374–84.

Vercellino M, Plano F, Votta B, Mutani R, Giordana MT, Cavalla P. Grey matter pathology in multiple sclerosis. J Neuropathol Exp Neurol 2005; 64: 1101–7.